PROCEEDINGS OF SPIE

SPIEDigitalLibrary.org/conference-proceedings-of-spie

Volume holographic spectral imaging

Zhenyu Li, Demetri Psaltis, Wenhai Liu, William R. Johnson, Gregory Bearman

Zhenyu Li, Demetri Psaltis, Wenhai Liu, William R. Johnson, Gregory Bearman, "Volume holographic spectral imaging," Proc. SPIE 5694, Spectral Imaging: Instrumentation, Applications, and Analysis III, (23 March 2005); doi: 10.1117/12.611350

SPIE.

Event: SPIE BiOS, 2005, San Jose, CA, United States

Volume holographic spectral imaging

Zhenyu Li[a], Demetri Psaltis[a], Wenhai Liu[b], William R. Johnson[c], Gregory Bearman[c]
[a]California Institute of Technology, 1200 East California Boulevard, Pasadena, CA, USA 91125
[b]Ondax Inc., 850 East Duarte Road, Monrovia, CA, USA 91016
[c]Jet Propulsion Laboratory, California Institute of Technology, 4800 Oak Grove Drive, Pasadena, CA, USA 91109

ABSTRACT

We report on a volume holographic imaging spectrometer (VHIS) system which allows retrieval of a scene's two-dimensional spatial information as well as its spectral information. This is performed using a transmission volume hologram and a simple rotary scanning mechanism. The system has the advantages of high spectral and spatial resolutions and the potential of single-shot, four-dimensional (3D spatial plus 1D spectral) imaging by recording multiple volume holograms in the same material. Also, due to the transmission diffraction geometry, the system automatically eliminates the stray excitation light from the captured signal. We give theoretical analysis of the performance and experimental demonstration using fluorescent CdSe/ZeS quantum dots. The measured quantum dots spectra agree well with the spectra obtained using a conventional spectrometer.

Keywords: Imaging spectrometers, volume holograms, stray excitation light, fluorescence spectroscopy, quantum dots

1. INTRODUCTION

Spectral imaging has demonstrated its usefulness in a wide variety of fields, including fundamental science such as biology, chemistry, and geology, as well as in industry with pollution monitoring, drug discovery, and clinical diagnostics. The central part of any spectral imaging system is a wavelength selective element, whether it be a filter wheel, an interferometer, or a tunable bandpass filter[1]. All these methods need some type of scanning mechanism, either spectral or spatial, to complete the image cube. Recently a computed-tomography based imaging spectrometer (CTIS)[2] has been implemented, which captures a scene's spatial and spectral radiance information in a single snapshot. CTIS uses a custom made diffractive optical element (DOE) as the wavelength selective element and requires post-capture computation to recover the image cube. Here we introduce volume holograms as a new type of wavelength selective element for spectral imaging. A volume hologram is a three-dimensional (3D) phase grating in a volume medium. It is created by recording the interference pattern of two mutually coherent light beams. The 3D nature of volume holograms offers unique properties such as high diffraction efficiency (close to 100% at a single wavelength), high angle and spectral selectivity, and the ability of multiplexing many holograms in the same volume. Such properties make volume holograms very attractive for spectroscopic and imaging applications. In this paper, we report on a spectral imaging system which uses a transmission volume hologram and a simple rotary scanning mechanism. We achieved spectral coverage from 378 to 774nm, which is limited by the mechanical constraint on the incident angle on the hologram. The predicted minimum spectral resolution is about $1cm^{-1}$ (~0.03nm at 550nm) and the spatial resolution can be diffraction-limited using high magnification optics. Furthermore, due to the transmission diffraction geometry, the system automatically eliminates the stray excitation light. Finally, this technique holds the potential of realizing simultaneous four-dimensional (3D spatial plus 1D spectral) imaging by multiplexing several holograms in the same material.

2. TRANSMISSION VOLUME HOLOGRAMS

2.1. Bragg selectivity of transmission volume holograms

Two different theories are generally used to study the diffraction of light from volume holograms. In the weak grating regime, which means higher-order scattering by the hologram is negligible, the first Born's approximation[3] is often used to predict the diffraction efficiency of a volume hologram. However, in the strong grating regime, the Born's

Spectral Imaging: Instrumentation, Applications, and Analysis III, edited by
Gregory H. Bearman, Anita Mahadevan-Jansen, Richard M. Levenson, Proc. of SPIE
Vol. 5694 (SPIE, Bellingham, WA, 2005) · 1605-7422/05/$15 · doi: 10.1117/12.611350

approximation breaks down and coupled wave theory[4] must be applied. Since we use volume holograms which operate in the weak grating regime, we only give the first Born's approximation analysis.

Under the first Born's approximation, the diffracted optical field from a transmission volume hologram as shown in Figure 1 is given by[3]

$$E_D \propto \mathrm{sinc}\left(\frac{L(\mathbf{k}_P + \mathbf{K}_G - \mathbf{k}_D)\cdot\hat{z}}{2\pi}\right) = \mathrm{sinc}\left(\frac{L\Delta\mathbf{k}_z}{2\pi}\right) \tag{2.1}$$

where $\mathbf{k}_P$, $\mathbf{K}_G$, and $\mathbf{k}_D$ are the incident wave vector, grating vector, and the diffracted wave vector respectively. L is the hologram thickness. $\Delta\mathbf{k}_z$ equals $\mathbf{k}_P + \mathbf{K}_G - \mathbf{k}_D$. The diffraction efficiency, which is defined as the portion of incident intensity diffracted by the hologram, is therefore

$$\eta \propto \mathrm{sinc}^2\left(\frac{L\Delta\mathbf{k}_z}{2\pi}\right) \tag{2.2}$$

When $\mathbf{k}_P + \mathbf{K}_G = \mathbf{k}_D$, i.e. $\Delta\mathbf{k}_z = 0$, we get the maximum diffraction efficiency. This is the so-called *Bragg matching condition*. In the wave-vector space (**K**-sphere) diagram, this means $\mathbf{k}_P$, $\mathbf{K}_G$, and $\mathbf{k}_D$ form a closed triangle as shown in Figure 1. We call the quantity $\Delta\mathbf{k}_z$ the *Bragg mismatch factor*, which can be caused by angular or wavelength detuning from the Bragg matching condition.

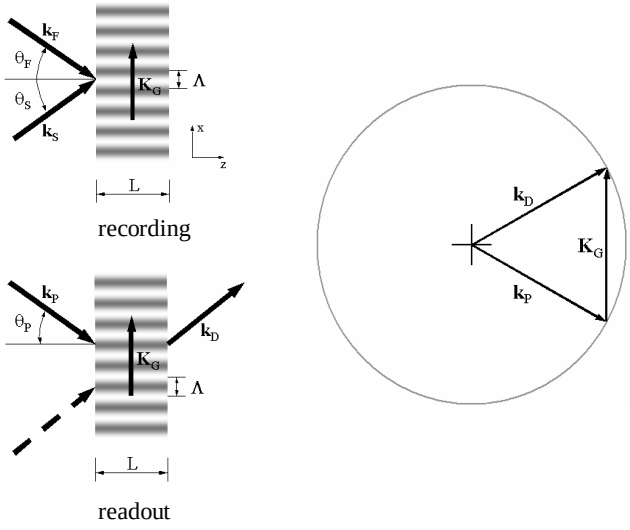

Figure 1. (left) Recording and readout of a transmission volume hologram, and (right) the corresponding wave-vector space diagram.

When the Bragg mismatch is due to the angular detuning $\Delta\theta$, the diffraction efficiency of a transmission volume hologram is given by

$$\eta \propto \mathrm{sinc}^2\left(\frac{2L\sin\theta}{\lambda}\Delta\theta\right) \tag{2.3}$$

where λ is the wavelength in the medium and θ is the Bragg-matched incident angle in the medium. The angular spacing between the central peak and the first null of the sinc function is referred to as the *angle Bragg selectivity*, and is given by

$$\Delta\theta_B = \frac{\lambda}{2L\sin\theta} \tag{2.4}$$

A measured angle selectivity curve of a hologram recorded in a 3mm thick PQ-PMMA photopolymer (n=1.5) is shown in Figure 2. When the Bragg mismatch comes from the wavelength detuning $\Delta\lambda$, the diffraction efficiency is

$$\eta \propto \mathrm{sinc}^2\left(\frac{2L\sin^2\theta}{\lambda^2\cos\theta}\Delta\lambda\right) \tag{2.5}$$

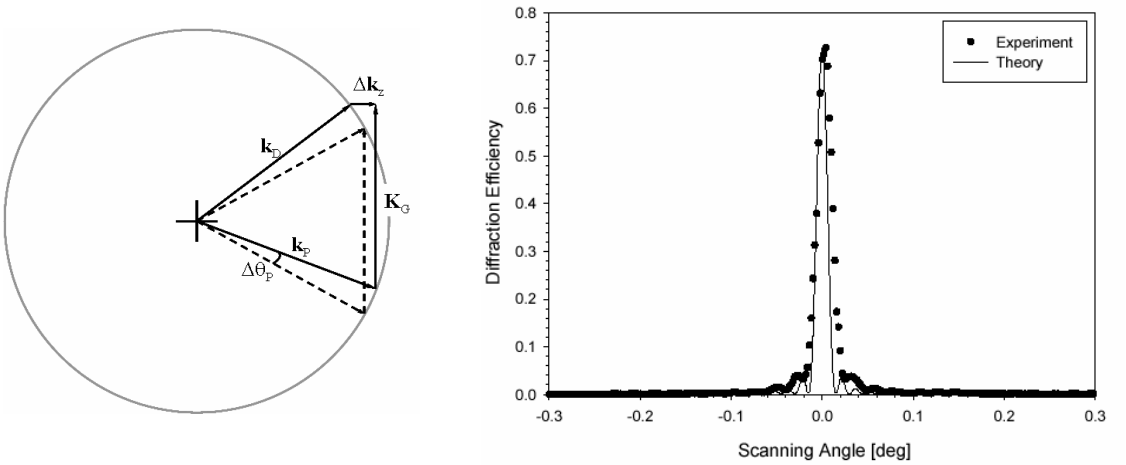

Figure 2. Experimental angle selectivity curve of a volume hologram recorded in a 3mm thick PQ-PMMA with incident angle $\theta = 30^o$ (dots) and the theoretical prediction (solid line).

And the corresponding *wavelength Bragg selectivity* is given by

$$\Delta\lambda_B = \frac{\lambda^2 \cos\theta}{2L\sin^2\theta} \text{ (in the medium)} \qquad (2.6)$$

The calculated wavelength selectivity curve of a 3mm thick volume hologram with an incident angle of 45 ^{o} ($\theta = 45^o$) in a photosensitive glass (n = 1.5) is plotted in Figure 3. As we can see, at the operation wavelength λ = 550nm, very narrow wavelength selectivity 0.03nm can be achieved, which corresponds to a resolving power over 18000.

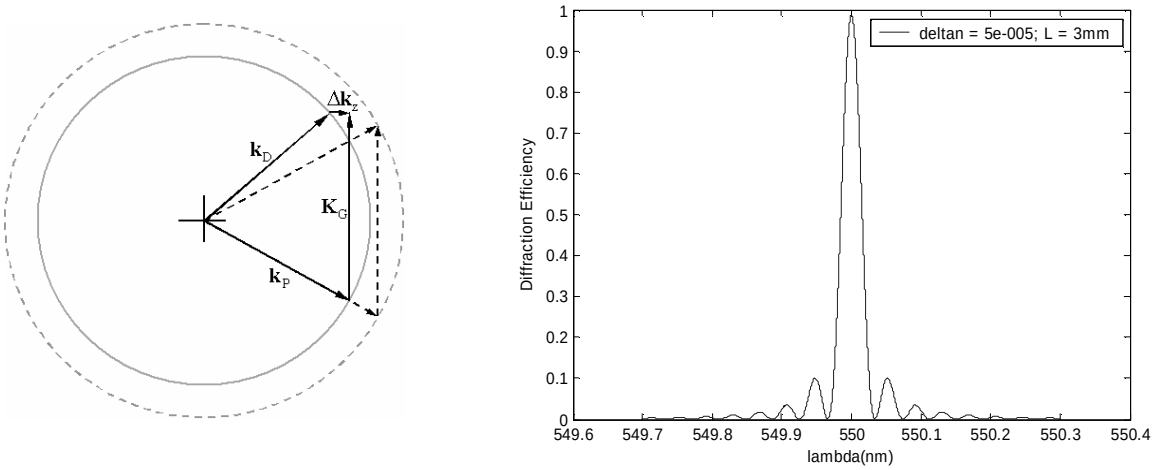

Figure 3. Bragg mismatch due to the wavelength detuning and the corresponding wavelength selectivity curve of a volume hologram recorded in a 3mm thick a photosensitive glass with an incident angle of 45 ^{o} ($\theta = 45^o$). The operation wavelength is 550nm.

2.2. Bragg degeneracy properties of volume holograms

Bragg degeneracy means Bragg matching with a probe beam that is different from the recording beams. Two types of Bragg degeneracies exist in the transmission geometry. From the Bragg matching condition given above, we know that any wave-vector pairs are Bragg matched when $\mathbf{k}_D - \mathbf{k}_P = \mathbf{K}_G$. The first Bragg degeneracy is obtained by rotation of the probe-diffracted wave-vector pair ($\mathbf{k}_P$, $\mathbf{k}_D$) around $\mathbf{K}_G$ while keeping the wavelength constant, as shown in Figure 4. We call this degeneracy wave-vector rotating degeneracy. The second degeneracy is for wave-vector pairs ($\mathbf{k}_P$, $\mathbf{k}_D$) at different wavelengths. Since in this case the incident angle of the probe beam needs to change according to the wavelength change, as shown in Figure 5, we call it angle-wavelength coupling degeneracy. VHIS employs these two degeneracies to achieve slicing of the 3D image cube.

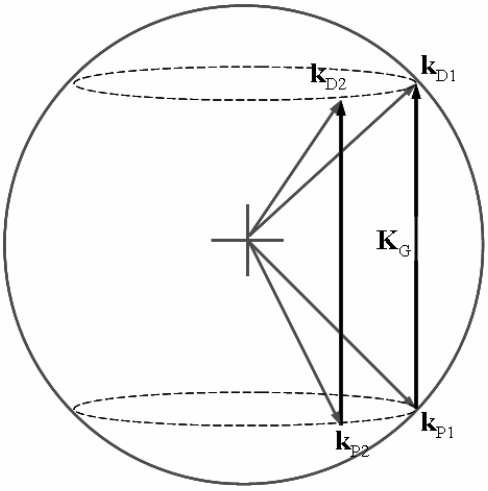

Figure 4. Wave-vector rotating Bragg degeneracy.

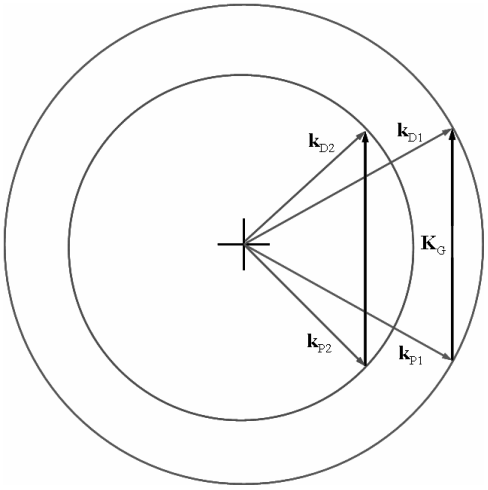

Figure 5. Angle-wavelength coupling Bragg degeneracy.

3. EXPERIMENTAL METHODS AND PERFORMANCE ANALYSIS

3.1. Experimental setup

The experimental setup of VHIS is shown in Figure 6. The quantum dots sample was excited by a commercial UV lamp with a peak irradiance output at 360nm. The fluorescent emission was collected by the 2:1 demagnification lens pair whose function was to fit the whole sample into the field of view (FOV). An achromatic lens (f = 100mm) collimated the incident light on to the volume hologram. The hologram diffracted light according to the Bragg matching condition. The diffracted light was collected by another lens (f = 80mm) and focused onto a CCD. The volume hologram and the imaging arm (imaging lens and CCD) were mounted on two co-axial rotation stages, since the imaging arm must be rotated by an angle 2θ when the volume hologram is rotated by θ. The y-dimensional information was captured by the wave-vector rotating degeneracy of the hologram. The x-dimensional information was captured by the angle-wavelength coupling degeneracy, which means every position along x shows up as a different color on the CCD. Therefore, each image forms a rainbow slicing of the 3D image cube. By rotating the grating and imaging arm together, the scanning along the wavelength dimension was achieved. A scanning step of 0.8^o corresponds to about 10nm shift in wavelength at 550nm.

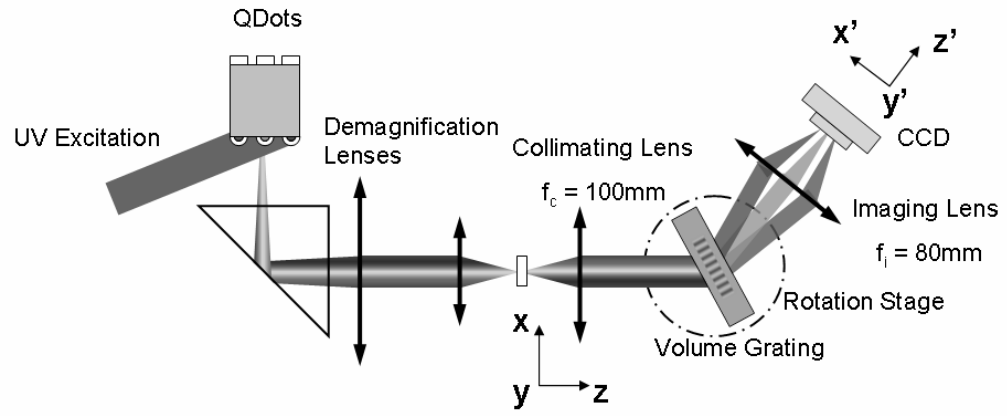

Figure 6. Experimental setup of the volume holographic imaging spectrometer (VHIS). When the volume grating is rotated by angleθ, the imaging lens and CCD needs to be rotated by 2θ.

The volume hologram was recorded in a proprietary photosensitive glass from Ondax Inc. The dimensions of the glass are 30mm×10mm×3mm, which gives a large enough aperture for most imaging applications. The measured diffraction efficiency at 488nm is about 70%. The Bragg-matched incident angle is 45^0 at 632nm. A commercially available, scientific grade, CCD camera was used with a local computer for all data recording. It had a 1024x1024 detector array and 10-bit digitization. The camera provided low noise imaging, fast response time and fine spatial sampling (8x8μm pitch). The broadband UV fluorescent lamp provided adequate and uniform illumination across the small 25x25 mm sample region which in turn allowed the quantum dots to fluoresce in the visible. A total of 6 different CdSe/ZnS core-shell quantum dot samples in toluene were purchased through a commercial supplier (Evident Technologies) and mixed in situ to create concentrations which encouraged similar flux level fluorescent output when UV excitation was present. Each sample was labeled accordingly by its apparent fluorescence color (A - Adirondack Green, B - Catskill Green, C - Hops Yellow, D - Birch Yellow, E - Fort Orange, F - Maple Red-Orange). For spatial-spectral verification, we used the CTIS[2] to measure the emission spectra of the sample. Figure 7 shows a spatial raster and legend of the field of view along with the CTIS measured spectra of the six quantum dots solutions used. Each spectrum has been normalized and shows some expected FWHM broadening due to the CTIS iterative algorithmic retrieval methods. Some response at lower wavelengths for E and F is due to cross refraction of the individual holder elements (glass material) and was corrected with proper baffling.

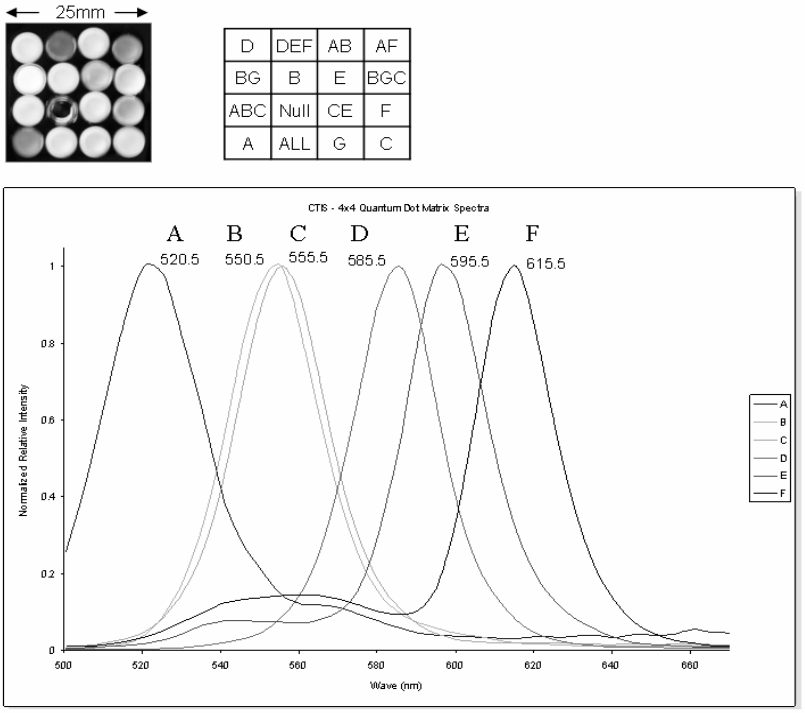

Figure 7. Fluorescent image and CTIS measured spectra of the CdSe/ZeS quantum dots sample.

3.2. Performance analysis

The realizable incident angle on the hologram is from 25^o to 60^o due to mechanical constraints, which corresponds to a spectral coverage from 378 to 774nm. The spectral bandpass of the hologram is determined by the wavelength Bragg selectivity, which is about $1cm^{-1}$ (~0.03nm at 550nm) calculated using Eq. 2.6. However the achievable spectral resolution is limited by the minimum angle step of the rotation stage. The minimum step of our rotation stage is 0.01^o, which gives $4.1cm^{-1}$ (~0.125nm at 550nm) spectral resolution. The real spectral resolution is determined by the used scanning step. For example, a scanning step of 0.8 degree corresponds to about $330cm^{-1}$ resolution (~10nm at 550nm). The spatial resolution along x dimension is given by the angle Bragg selectivity (Eq. 2.4) of the hologram multiplied by the focal length of the collimating lens. This gives about 30um resolution for the current system which uses a 100mm focal length collimating lens. This resolution can be substantially increased by using a short focal length microscope objective. A 100X objective with 1.8mm focal length gives about 0.5um resolution, which means this resolution becomes diffraction-limited by the optics rather than by the hologram. The spatial resolution along y direction is

diffraction-limited by the imaging optics because no angle Bragg selectivity exists along this direction. The aperture size of the hologram is 30mm×10mm, which currently limits FOV of the system. The maximum scanning speed is limited by the rotation stage to 80°/second, corresponding to ~1nm/ms at 550nm. The throughput is expected to be low because of the extremely narrow bandwidth and polarization sensitivity of the hologram. However, the diffraction efficiency of the hologram at a single wavelength is about 70%. As mentioned before, the stray excitation light and out-of-band noise are highly reduced due to the high spectral selectivity of the hologram and the transmission diffraction geometry.

4. RESULTS AND DISSCUSION

A series of captured images of the quantum dots sample are shown in Figure 8. Due to the angle-wavelength coupling degeneracy of the hologram, each image is a rainbow image with longer wavelength on the left. The wavelength range inside FOV is shown on top of each image, which decreases from 75.6 to 63.7nm with increasing wavelength. The spectra of solution DEF measured by VHIS and CTIS are shown in Figure 9, in which the VHIS data is after correcting the wavelength dependence of the hologram diffraction efficiency and FOV, and the CCD spectral response. It is clear that the two spectra show good agreement between VHIS and CTIS measurements. Other performance features such as spatial resolution, spectral resolution, throughput, out-of-band rejection, and max scanning speed are under investigation.

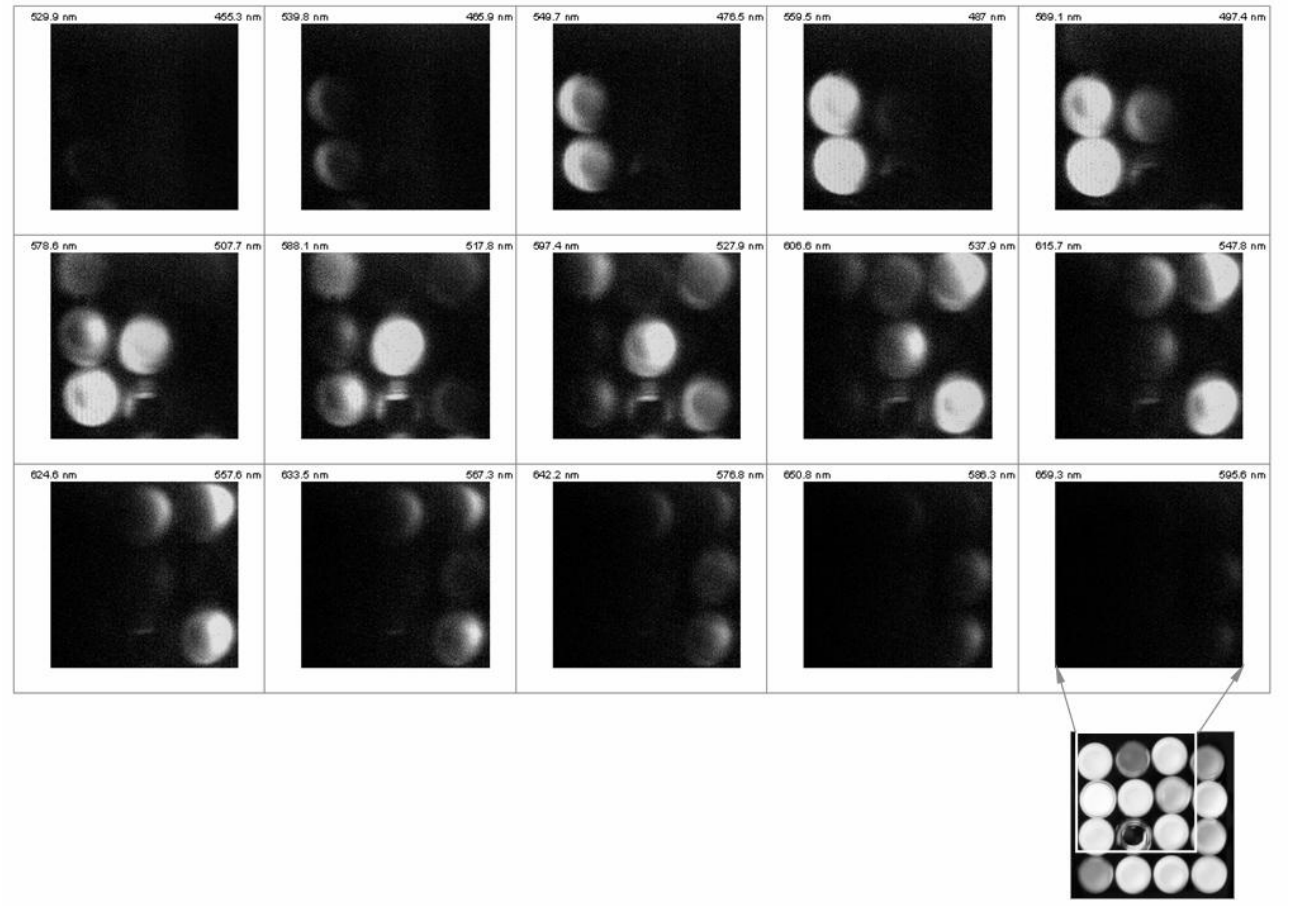

Figure 8. VHIS captured raw images. Scanning step is 0.8 degree (~10nm at 550nm).

5. CONCLUSION

We have demonstrated a transmission volume hologram based spectral imaging system. The system uses a simple rotary scanning mechanism to scan the wavelength space. The achieved spectral range covers near UV 378nm to near IR 774 nm and is limited by the mechanical constraint on the incident angle on the hologram. Both high spectral

resolution 1cm^{-1} and spatial resolution (diffraction-limited) can be achieved according to the theoretical analysis. Furthermore, good signal-to-noise ratio is achievable since the stray excitation light and out-of-band noise are automatically eliminated due to the high spectral selectivity of the hologram and the transmission diffraction geometry.

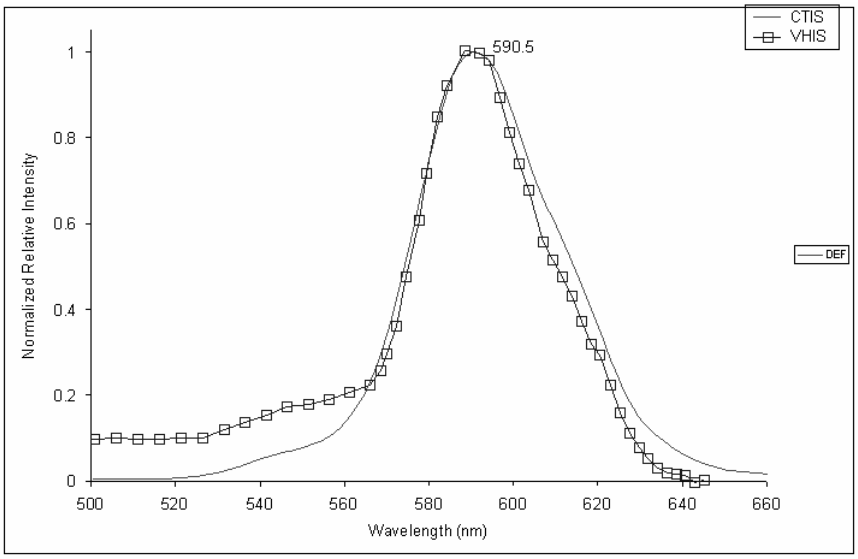

Figure 9. The spectra of solution DEF measured by VHIS and CTIS.

However, compared to other spectral imaging techniques, perhaps the most attractive feature of volume holograms is the potential of realizing single shot spectral imaging without post-capture computation. This can be accomplished by multiplexing several tens of holograms in the same material. Each hologram diffracts light in a narrow spectral band to a distinct direction so that image slices at different wavelengths can be projected onto different areas of the same detector. Recently we have demonstrated a multi-line holographic filter for spectroscopy with seven strong holograms (average diffraction efficiency ~60%) recorded in an iron doped $LiNbO_3$ crystal[5]. This multiplexing capability has also been exploited for multi-depth imaging[6]. A new VHIS system with multiplexed holograms (thus no or little scanning) is currently under construction. The ultra-high spectral selectivity and multiplexing capability make this technique well suited for vibrational spectral imaging such as Raman and coherent anti-Stokes Raman scattering (CARS) imaging. In addition the multiplexing capability may find applications in fluorescence resonance energy transfer (FRET) with multiple donors and acceptors.

ACKNOWLEDGMENTS

This work was funded in part by a California Institute of Technology President's Fund and the Engineering Research Centers Program of the National Science Foundation under award EEC-9402726.

REFERENCES

1. G. Bearman, and R. Levenson, "Biological imaging spectroscopy", *Biomedical photonics handbook*, T. Vo-Dinh, Ed., CRC Press, 2003.

2. C.E. Volin, B.K. Ford, M.R. Descour, D.W. Wilson, P.M. Maker, and G.H. Bearman, "High speed spectral imager for imaging transient fluorescence phenomena", *Appl. Opt.* 37 (34), pp. 8112-8119, 1998.

3. G. Barbastathis and D. Psaltis, "Volume holographic multiplexing methods", *Holographic Data Storag*e, H. Coufal, L. Hesselink, and D. Psaltis, Eds. pp. 30-37, Berlin, Germany: Springer-Verlag, 2000.

4. H. Kogelnik, "Coupled wave theory for thick hologram gratings", *Bell Syst. Tech. J.* 48 (9), pp. 2909–2947, 1969.

5. H. Hsieh, Z. Li, and D. Psaltis, “Holographic filters”, *Organic Holographic Materials and Applications II,* Klaus Meerholz, Ed., Proc. SPIE 5521, pp. 24-28, 2004.

6. W. Liu, D. Psaltis, and G. Barbastathis, “Real-time spectral imaging in three spatial dimensions”, *Opt. Lett*. 27 (10), pp. 854-856, 2002.